Tikhonov regularization of instantaneous frequency attribute computations

Matthew J. Yedlin[1], Gary F. Margrave[2], Daryl Van Vorst[1], and Yochai Ben Horin[3]

ABSTRACT

We present a brief review of the concept of instantaneous frequency, obtained by differentiating the instantaneous phase, computed using the Hilbert Transform. This computation is recast as a Tikhonov regularized linear inverse problem and is compared with the alternative Fomel smoothing regularization. Both smoothing methods, and an equivalent frequency measure obtained via the normalized first moment of the spectrum of the Gabor Transform are applied to synthetic data, an earthquake and a quarry blast.

INTRODUCTION

As introduced by Nobel Laureate, Dennis Gabor (Gabor, 1946)the instantaneous frequency has been used as one of number of exploration seismology attributes, beginning in 1979 (Taner et al., 1979) and extended by Barnes (1992, 1993). The classical instantaneous frequency computation will be reviewed in the continuous domain and will be compared to the presentation of an alternate measure based on the first frequency moment of the Gabor transform spectrum as developed by Margrave (Margrave et al., 2005, 2011).

As the classic computation suffers form an instability, it will be reformulated as a Tikhonov-regularized inverse problem and compared with the smoothing method of Fomel (Fomel, 2007b) and the first frequency moment of the Gabor specturm. All three methods will be applied to synthetic data, an earthquake and a quarry blast.

THEORY

Classical Instantaneous Phase

The classical instantaneous phase originates with phase modulation concepts (Boashash, 1992a,b), with the underlying assumption that the signal is basically a complex exponential, with a small deviation about a carrier frequency, ω_0. This concept can be generalized to a general complex signal, known as the analytic signal, given by

$$A(t) = f(t) + i\mathcal{H}[f(t)] = f(t) + ig(t) \tag{1}$$

where $g(t)$ is obtained by the Hilbert transform, a convolution operation defined by

$$g(t) = \int_{-\infty}^{\infty} f(\tau)\,\frac{1}{\pi(t-\tau)}\,d\tau. \tag{2}$$

[1]Department of Electrical and Computer Engineering, University of British Columbia
[2]Geoscience, University of Calgary
[1]Department of Electrical and Computer Engineering, University of British Columbia
[3]SOREQ Nuclear Research Center (SNRC), Yavneh, Israel

Basically the Hilbert transform maps cosines into sines and sines into negative cosines, resulting in positive frequency Fourier transform components phase-delayed by $\frac{\pi}{2}$ and negative frequency components phase-advanced by $\frac{\pi}{2}$.

From (1), $A(t)$ can be written in polar form with magnitude $Env(t)$ and phase, $\Phi(t)$ given by

$$\begin{aligned} A(t) &= f(t) + ig(t) = Env(t)\ \exp\left[i\Phi(t)\right], \quad \text{where} && (3)\\ Env(t) &= \sqrt{f(t)^2 + g(t)^2}, \quad \text{and} && (4)\\ \Phi(t) &= \tan^{-1}\left[\frac{g(t)}{f(t)}\right] && (5) \end{aligned}$$

with

$$\begin{aligned} f(t) &= Env(t)\ \cos[\Phi(t)], \quad \text{and} && (6)\\ g(t) &= Env(t)\ \sin[\Phi(t)]. && (7) \end{aligned}$$

We can differentiate (5) with respect to time by simple application of the chain rule to obtain the instantaneous angular frequency (IAF), $\Omega(t)$, given by

$$\Omega(t) = \frac{d\,\Phi(t)}{dt} = \frac{n(t)}{d(t)} = \frac{f(t)\frac{d}{dt}g(t) - g(t)\frac{d}{dt}f(t)}{f(t)^2 + g(t)^2}. \tag{8}$$

This estimate is divided by 2π to obtain the instantaneous frequency. There is a clear instability in (8) due to the denominator becoming very small. This instability is amplified by the fact that we have differentiated and subtracted the product of two time series. At the heart of the foregoing issues is the elementary, but paradoxical fact: there is no such thing as instantaneous frequency and we definitely need a time-interval to estimate frequency. As such we need to focus on local, or localized frequency, which we denote by f_{loc}.

Computation of the local Frequency, f_{loc}, via a First Frequency Moment

An alternative to the direct computation of the local frequency which avoids differentiation is provided in the book by Cohen (Cohen, 1995). He presents an estimate of the local frequency by taking the frequency moment of employing the spectrum of the time-frequency transform. Thus the local frequency, f_{loc}, which we will use in the section **Applications**, is given in continuous time, by

$$f_{loc} = \frac{1}{\int |S(t,f)|^2\, df} \int |f|\, |S(t,f)|^2\, df. \tag{9}$$

In (9), the time-frequency transform, $S(t,f)$, can be computed using either the Gabor transform or other time-frequency transforms such as the Stockwell transform. The Gabor transform, $S_{Gabor}(t,f)$, used in this study is given by

$$S_{Gabor}(t,f) = \int_{-\infty}^{\infty} g(\tau)\ win(\tau - t) e^{-i\,2\pi f \tau} d\tau \tag{10}$$

where $g(t)$ is our seismic trace, and in (10), $win(t)$ is chosen to be a fixed-width Gaussian window. For the moment computation, the integrals are performed over the signal bandwidth.

Local Frequency via Tikhonov Regularization

The problem of the instability of the calculation of the instantaneous frequency can be addressed by rewriting it in classical linear form,

$$\mathbf{A}\mathbf{f}_{\mathbf{inst}} = \frac{1}{2\pi}\mathbf{d} = \tilde{\mathbf{d}} \tag{11}$$

In (11), $\mathbf{d}$ is the discrete vector of the numerator of the right hand side of (8), $\mathbf{f_{inst}}$ is the vector of estimated instantaneous frequency and $\mathbf{A}$ is a diagonal matrix whose elements are the discrete values of the envelope squared. The instability problem is clearly evident and requires the abandonment of the classical concept of instantaneous frequency in favor of the smoother version, which we defined previously as f_{loc}.

Fomel (2007a,b), has addressed this issue by solving a smoothed problem in which a constrained least squares technique is used, based on previous work by Claerbout (Fomel and Claerbout, 2003). Fomel regularizes the formulation in (11) by relating the regularization operator $\mathbf{R}$ in terms of a smoothing operator $\mathbf{S}$, as

$$\mathbf{S} = \left(\mathbf{I} + \epsilon^{\mathbf{2}}\mathbf{R}\right)^{-\mathbf{1}}. \tag{12}$$

He then computes the local frequency, $\mathbf{f_{loc}}$, as

$$\mathbf{f_{loc}} = \left[\lambda^{\mathbf{2}}\mathbf{I} + \mathbf{S}\left(\mathbf{A} - \lambda^{\mathbf{2}}\mathbf{I}\right)\right]^{-\mathbf{1}}\mathbf{S}\tilde{\mathbf{d}}, \tag{13}$$

where λ is a scaling factor.

As an alternative of Fomel's development for $\mathbf{f_{loc}}$, we use the explicit Tikhonov regularization employed in linear inverse theory to recast (11) as the least squares problem,

$$\underset{\mathbf{f_{loc}}}{\text{minimize}}\left\|\mathbf{A}\mathbf{f_{loc}} - \tilde{\mathbf{d}}\right\|^2 + \lambda^2\|\mathbf{W}\mathbf{f_{loc}}\|^2. \tag{14}$$

In (14), λ is the Tikhonov regularization parameter and $\mathbf{W}$ is a matrix operator that determines the type of model that we choose. In this analysis, for the numerical examples, we will, choose $\mathbf{W}$ to be a bidiagonal matrix that represents the first derivative, yielding the smoothest model, $\mathbf{f_{loc}}$, for a particular choice of λ.

EXAMPLES

We now consider the computation of the localized frequency, f_{loc} for three data sets:

1. A synthetic trace;
2. An earthquake in the Gulf of Suez;

3. A quarry blast in Jordan.

In all cases the localized frequency f_{loc} will be presented in units of Hz and will be computed using the Tikhonov regularized solution to the minimization of (14), the Fomel method as given by (13) and the first moment calculation given by (9).

Synthetic trace

We begin our examples by considering the synthetic trace

$$s(t) = e^{-.05t}cos(2\pi t) + (1 - e^{-.05t})cos(2\pi 5t). \tag{15}$$

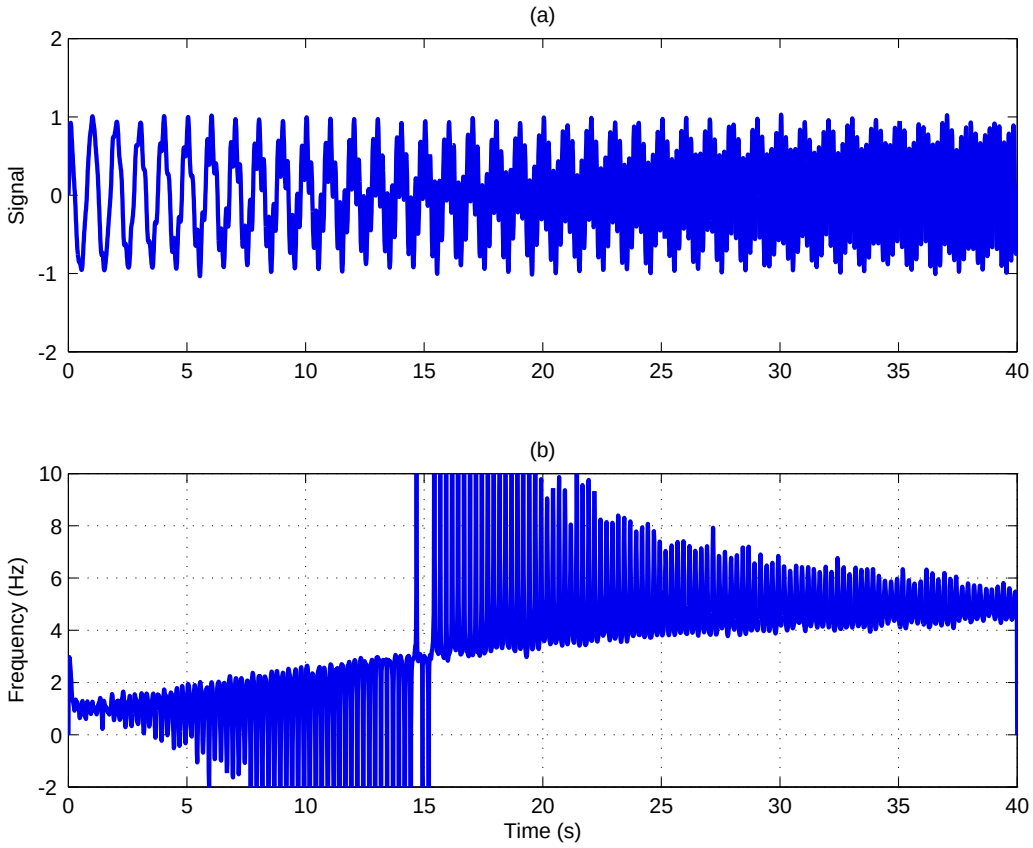

FIG. 1. Panel (a) Signal given by $s(t) = e^{-.05t}cos(2\pi t) + (1 - e^{-.05t})cos(2\pi 5t)$.
Panel (b) Classical instantaneous frequency with no regularization.

In Panel (a) of Fig. 1, we see the noisy interlaced sinusoids, with the instantaneous frequency shown in Panel (b), which is the classical instantaneous frequency. It is highly unstable, with a hint of the correct answer if we consider only the envelope. Confirmation of this is shown in Fig. 2.

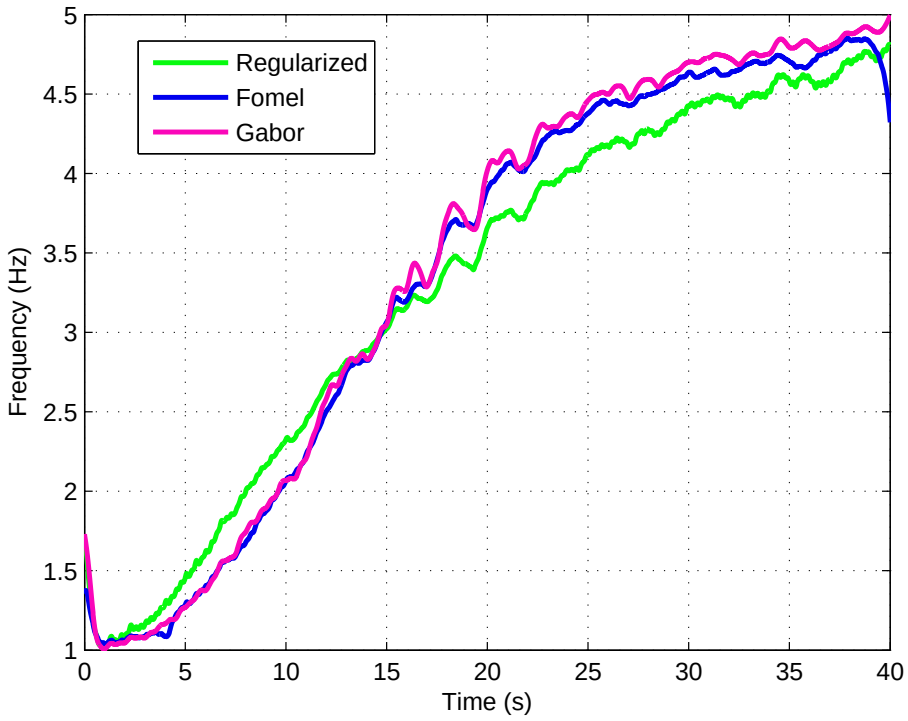

FIG. 2. Comparison of the Tikhonov, Fomel and Gabor first moment algorithms for computing f_{loc}.

We note that all three techniques provide a very good description of the continual variation of the computation of f_{loc} from 1 to 5 Hz, with the Fomel and Gabor first moment techniques yielding virtually the same result. What is surprising is that the result for the Tikhonov-regularized algorithm, based on the classical instantaneous frequency calclulation in (8), is within 10 % of the Gabor and Fomel results over the entire signal duration. The regularization parameter was initially estimated using the l-curve method (Hansen and O'Leary, 1993; Wu, 2003) and then was manaully adjusted.

Gulf of Suez Earthquake

We begin our analysis of real data by considering a local earthquake located in the Gulf of Suez ($29.24°N, 32.76°E$). The earthquake was recorded on 2014/09/10 at the station EIL($29.67°N, 34.95°E$) and had a local magnitude of 2.2, as computed by the Geophysical Institute of Israel's duration-based local magnitude scale. We will sequentially present all three components of the recording, E(East), N(North) and Z beginning with the east component.

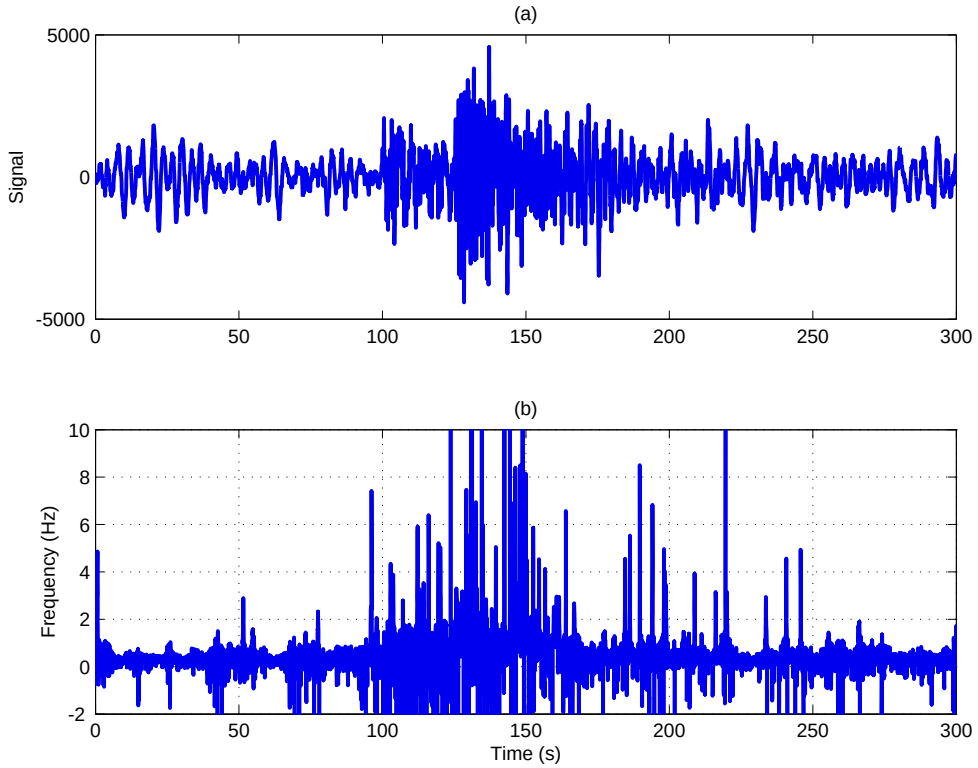

FIG. 3. Gulf of Suez Earthquake. (a) East component recording. (b) Classical instantaneous frequency

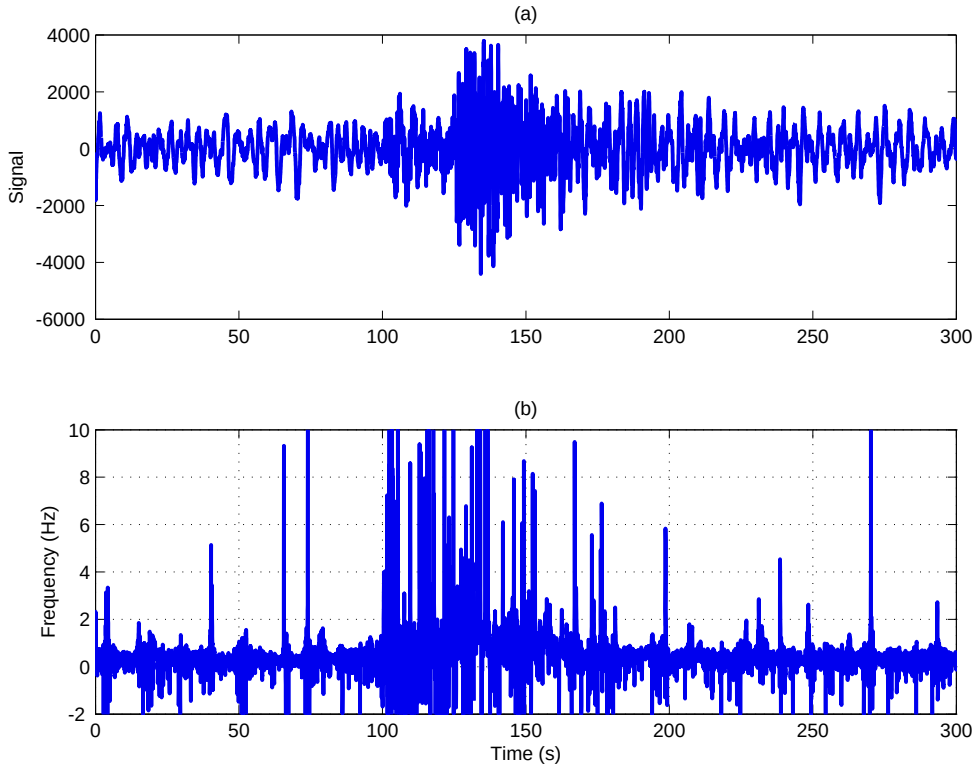

FIG. 4. Gulf of Suez Earthquake. (a) North component recording. (b) Classical instantaneous frequency

In Fig. 3, Fig. 4, and Fig. 5 panel (a) is the recorded signal and panel (b) is the in-

stantaneous frequency as computed using (8). It is clear that the classical instantaneous frequency exhibits a catastrophic failure for the E, N and Z components. In panel (a) of all the figures, we can see the onset of the P-wave at 100 sec. and the onset of the S-wave at 125 sec.

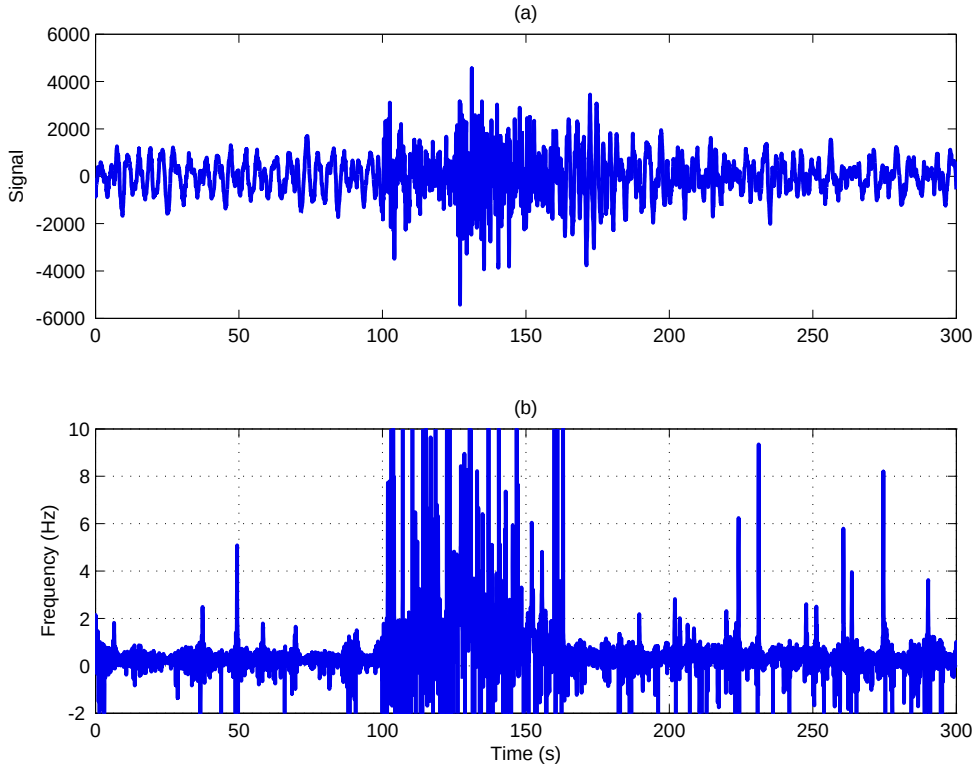

FIG. 5. Gulf of Suez Earthquake. (a) Z component recording. (b) Classical instantaneous frequency

For each of the three foregoing components, we will now present the calculation of f_{loc} using the Tikhonov regularized formulation, Fomel smoothing and the first frequency moment of the Gabor power spectrum. In all the following figures, Fig. 6,Fig. 7, and Fig. 8,the onset of both the P and S waves is much clearer. What is amazing is the consistency of the f_{loc} traces for each component!

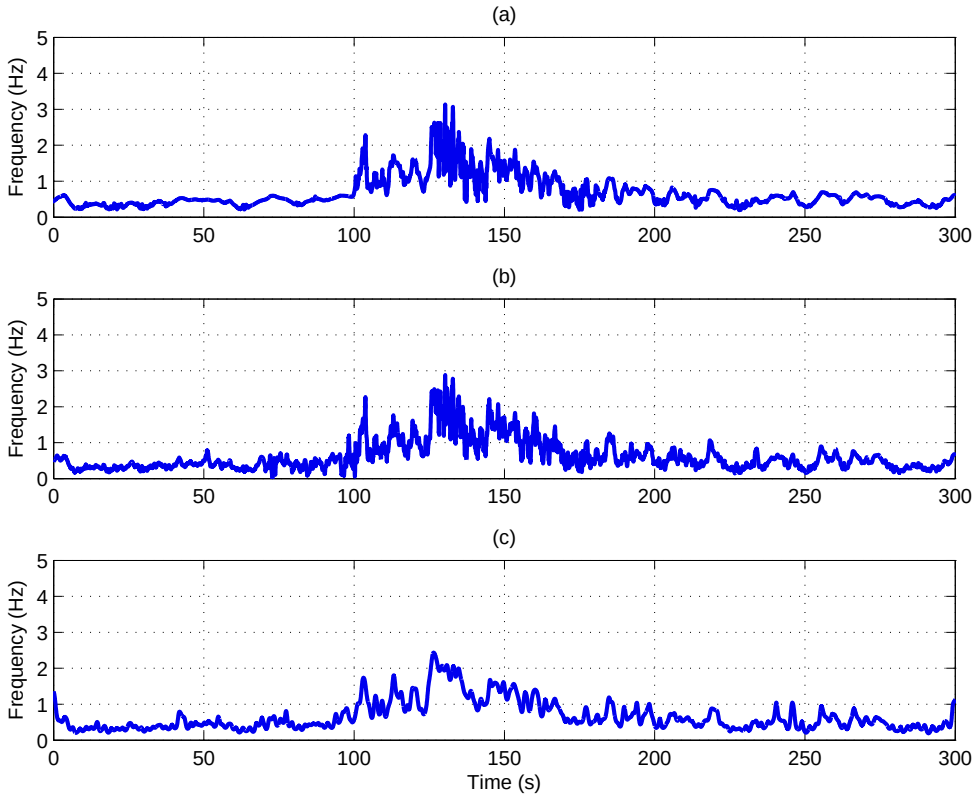

FIG. 6. E component $\mathbf{f_{loc}}$ results. (a) Tikhonov regularization. (b) Fomel smoothing. (c) Gabor spectrum frequency moment.

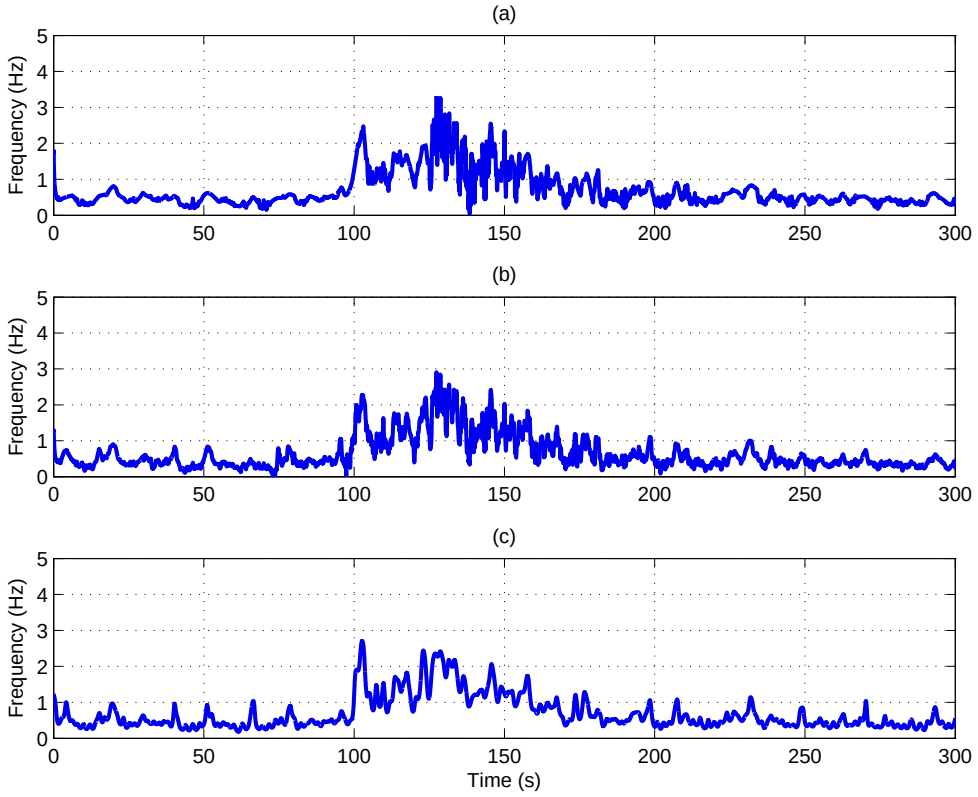

FIG. 7. N component $\mathbf{f_{loc}}$ results. (a) Tikhonov regularization. (b) Fomel smoothing. (c) Gabor spectrum frequency moment.

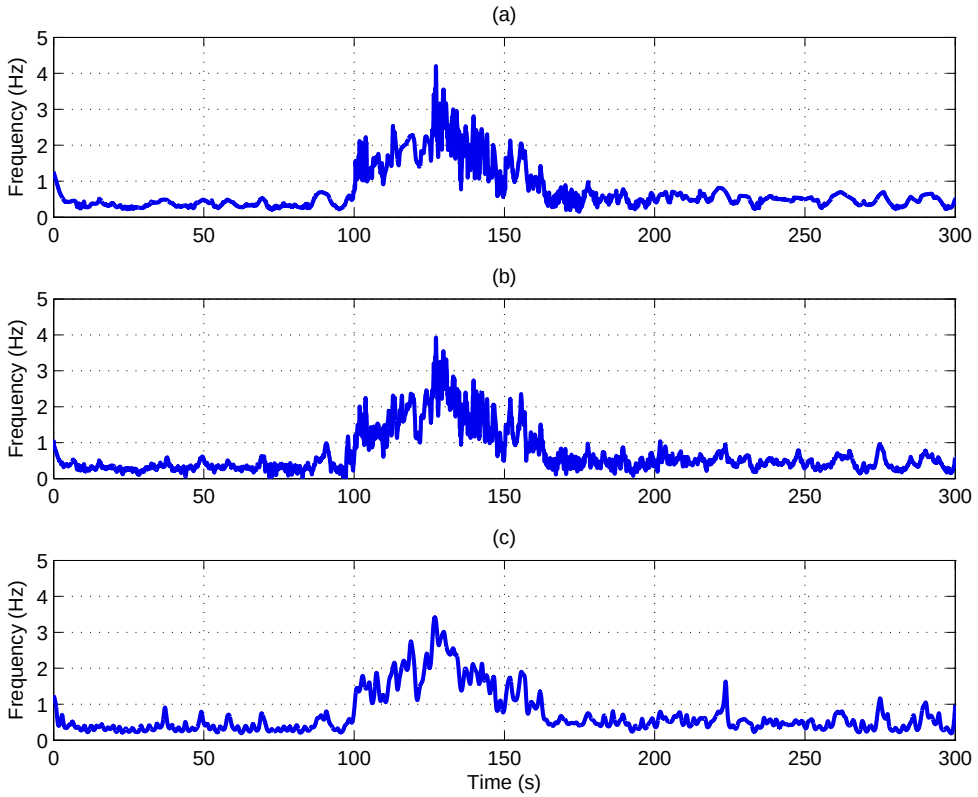

FIG. 8. Z component $\mathbf{f_{loc}}$ results. (a) Tikhonov regularization. (b) Fomel smoothing. (c) Gabor spectrum frequency moment.

Jordanian Quarry Blast

We continue our analysis of real data by considering a local quarry blast located in Jordan ($36.18°N, 31.05°E$). The blast was recorded on 2014/09/09 at the station EIL ($29.67°N, 34.95°E$) and had a crude local magnitude of 1.8, as estimated using the maximum distance to the recording stations. We will sequentially present all three components of the recording, E(East), N(North) and Z, beginning with the east component.

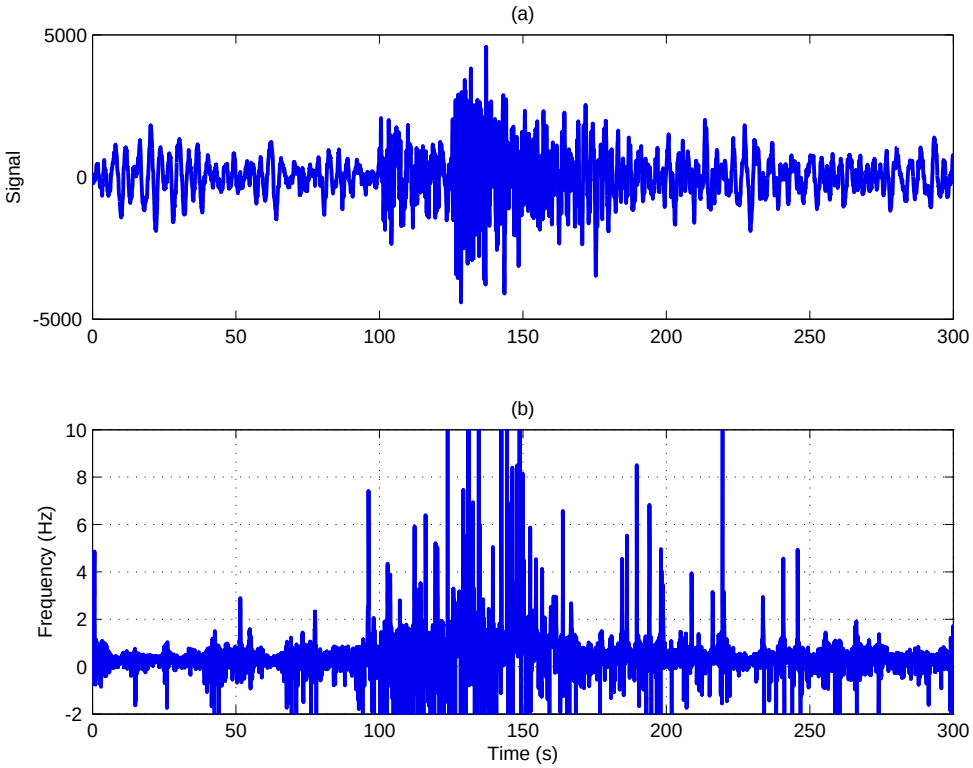

FIG. 9. Jordanian quarry blast. (a) East component recording. (b) Classical instantaneous frequency

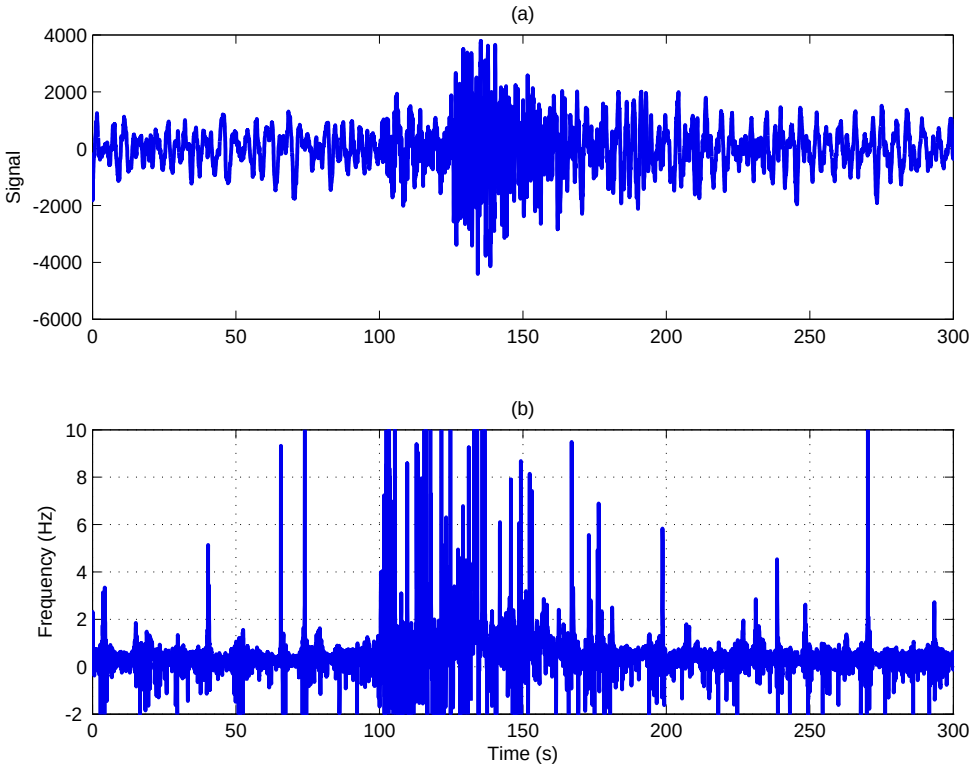

FIG. 10. Jordanian quarry blast. (a) North component recording. (b) Classical instantaneous frequency

In Fig. 9, Fig. 10, and Fig. 11 panel (a) is the recorded signal and panel (b) is the instan-

taneous frequency as computed using (8). It is clear again that the classical instantaneous frequency exhibits a catastrophic failure for the E, N and Z components. In panel (a) of all the raw data figures, we can see that it is difficult to pick the onset of the P and S waves.

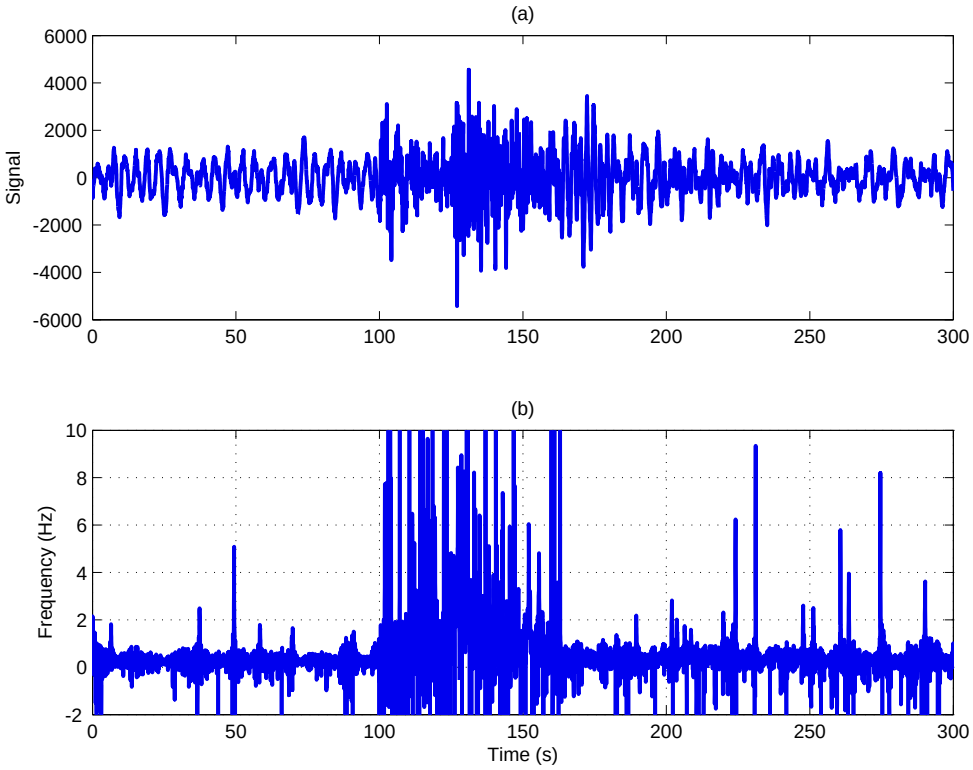

FIG. 11. Jordanian quarry blast. (a) Z component recording. (b) Classical instantaneous frequency

For each of the three foregoing components, we will now present the calculation of the local frequency using the Tikhonov regularized formulation, Fomel smoothing and the first frequency moment of the Gabor power spectrum. In all the following figures, Fig. 12, Fig. 13, and Fig. 14, the onset of both the P and S waves is much clearer than in the raw data, with the P wave onset at 80 sec. and the S wave onset at 110 sec. As before, for each component, all three methods provide a similar time-evolution of the local frequency.

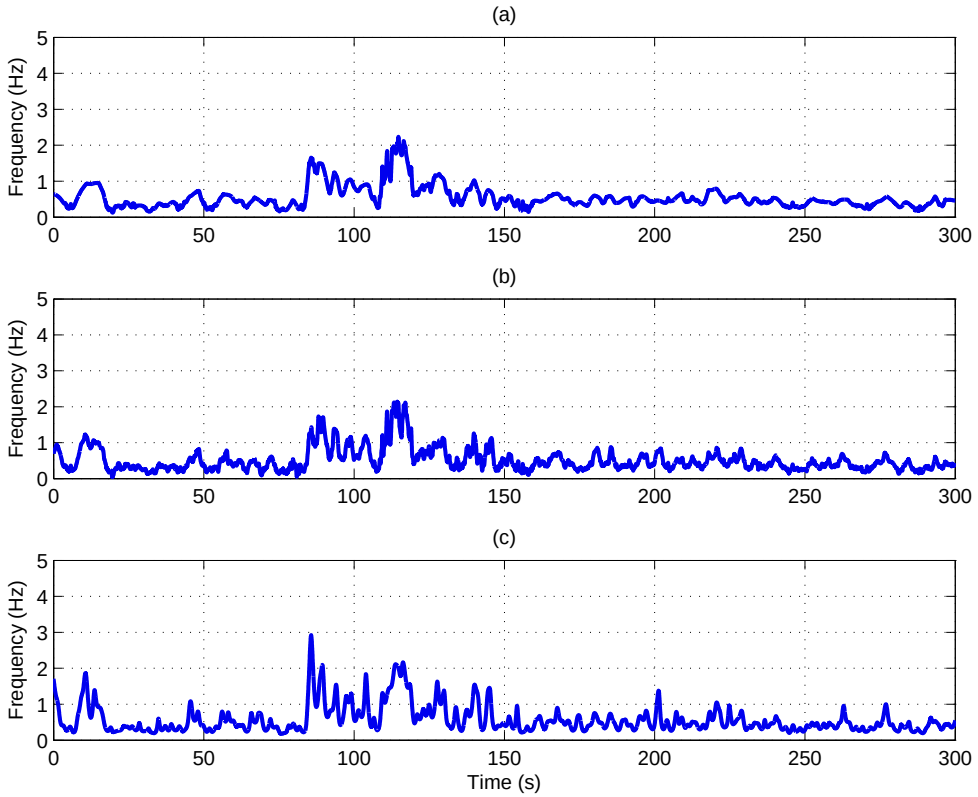

FIG. 12. E component $\mathbf{f_{loc}}$ results. (a) Tikhonov regularization. (b) Fomel smoothing. (c) Gabor spectrum frequency moment.

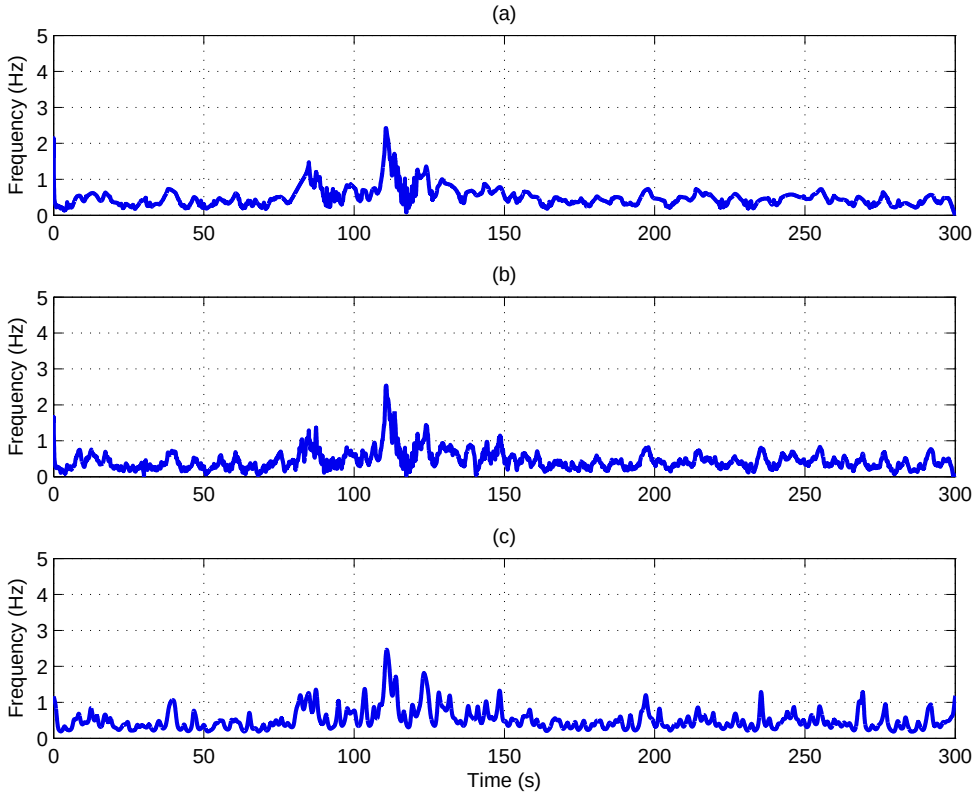

FIG. 13. N component $\mathbf{f_{loc}}$ results. (a) Tikhonov regularization. (b) Fomel smoothing. (c) Gabor spectrum frequency moment.

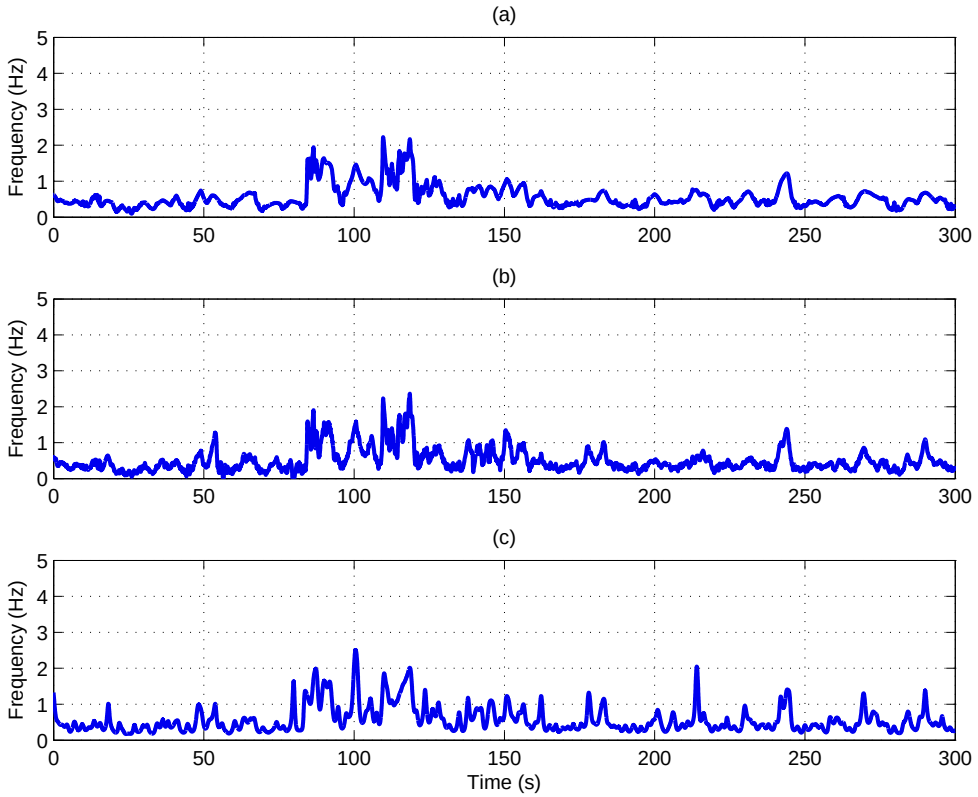

FIG. 14. Z component $\mathbf{f_{loc}}$ results. (a) Tikhonov regularization. (b) Fomel smoothing. (c) Gabor spectrum frequency moment.

CONCLUSIONS

An earthquake of local magnitude 2.2, located in the Gulf of Suez and a Jordanian quarry blast of local magnitude 1.8, recorded at the Israeli National Data Center location EIL, have been used to test the computation of a new attribute, f_{loc}, the local frequency. Three methods were used:

1. A Tikhonov regularized version of the classical instantaneous frequency attribute;
2. A smoothed version of the classical method based on a regularization technique devised by Fomel (Fomel, 2007b);
3. A frequency-moment method based on integration of the time-frequency spectrum obtained using the first frequency moment of the Gabor transform.

For all component of both datasets, the foregoing three methods all yielded very comparable results, even thoug the computational algorithms were vastly different. The fastest algorithm was the novel Tikhonov-regularized algorithm, which involved one FFT cycle, algebraic manipulation of the signal and its Hilbert transform, and the inversion of a tridiagonal matrix.

Future work will focus on on choosing the optimal regularization parameter of the Tikhonov method. In particular we will focus on the frequency-smoothing aspects of these

methods and their relation to other seismic data processing techniques, such as, for example, cepstral analysis.

ACKNOWLEDGEMENTS

We thank the sponsors of CREWES for their support. We also gratefully acknowledge support from NSERC (Natural Science and Engineering Research Council of Canada) through the grant CRDPJ 379744-08. We also thank NSERC providing an operating grant to M.Yedlin.

REFERENCES

Barnes, A. E., 1992, The calculation of instantaneous frequency and instantaneous bandwidth: Geophysics, **57**, No. 11, 1520–1524.

Barnes, A. E., 1993, Instantaneous spectral bandwidth and dominant frequency with applications to seismic reflection data: Geophysics, **58**, No. 3, 419–428.

Boashash, B., 1992a, Estimating and interpreting the instantaneous frequency of a signal. i. fundamentals: Proceedings of the IEEE, **80**, No. 4, 520–538.

Boashash, B., 1992b, Estimating and interpreting the instantaneous frequency of a signal. ii. algorithms and applications: Proceedings of the IEEE, **80**, No. 4, 540–568.

Cohen, L., 1995, Time-frequency analysis, vol. 778: Prentice Hall PTR New Jersey.

Fomel, S., 2007a, Local seismic attributes: Geophysics, **72**, No. 3, A29–A33.

Fomel, S., 2007b, Shaping regularization in geophysical-estimation problems: Geophysics, **72**, No. 2, R29–R36.

Fomel, S., and Claerbout, J. F., 2003, Multidimensional recursive filter preconditioning in geophysical estimation problems: Geophysics, **68**, No. 2, 577–588.

Gabor, D., 1946, Theory of communication. part 1: The analysis of information, part 2: The analysis of hearing, part 3: Frequency compression and expansion: Electrical Engineers - Part III: Radio and Communication Engineering, Journal of the Institution of, **93**, No. 26, 429–457.

Hansen, P. C., and O'Leary, D. P., 1993, The use of the l-curve in the regularization of discrete ill-posed problems: SIAM Journal on Scientific Computing, **14**, No. 6, 1487–1503.

Margrave, G. F., Gibson, P. C., Grossman, J. P., Henley, D. C., Iliescu, V., and Lamoureux, M. P., 2005, The gabor transform, pseudodifferential operators, and seismic deconvolution: Integrated Computer-Aided Engineering, **12**, No. 1, 43–55.

Margrave, G. F., Lamoureux, M. P., and Henley, D. C., 2011, Gabor deconvolution: Estimating reflectivity by nonstationary deconvolution of seismic data: Geophysics, **76**, No. 3, W15–W30.

Taner, M. T., Koehler, F., and Sheriff, R., 1979, Complex seismic trace analysis: Geophysics, **44**, No. 6, 1041–1063.

Wu, L., 2003, A parameter choice method for tikhonov regularization: Electronic Transactions on Numerical Analysis, **16**, 107–128.